The Extragalactic Infrared Background and its Cosmological Implications
IAU Symposium, Vol. 204, 2001
Martin Harwit and Michael G. Hauser, eds.

Galactic Far-Infrared Diffuse Emission

François Boulanger, Jean-Philippe Bernard, Guilaine Lagache, Bertrand Stepnik

Institut d'Astrophysique Spatiale, Université Paris XI, batiment 121, 91405 Orsay, France

Abstract. We review the present understanding of the interstellar dust contribution to the far-IR ($\lambda > 100\,\mu$m) sky emission. We show how the contribution from the distinct ISM components (HI, H_2, HII gas) are identified and characterized through spatial correlation with gas emission lines. We discuss the spectral energy distribution of the emission from cirrus dust associated with diffuse HI gas and from colder dust associated with molecular gas. We relate the drop in dust emission temperature from the diffuse interstellar medium to molecular gas to an evolution of dust affecting both the abundance of small dust grains and the far-IR emissivity of large grains.

1. Introduction

The Infrared Astronomical Satellite (IRAS) and the Cosmic Background Explorer (COBE) surveys have considerably improved our knowledge of dust properties and its spatial distribution over the high Galactic latitude sky. With the IRAS data it became clear that interstellar dust comprises small particles stochastically heated by the absorption of photons to temperatures higher than the equilibrium temperature of large grains. Far from heating sources, these small particles make the 12, 25 and a significant fraction of the 60 μm IRAS emission. Only in the 100 μm band does the emission come from large grains emitting at the equilibrium temperature set by the balance between heating and cooling. COBE extended the IRAS observations to the far-infrared/submillimeter emission. These data have been used to characterize the spectral energy distribution (SED) of the large grain emission and the dust/gas spatial correlation (Wright et al. 1991; Reach et al. 1995; Boulanger et al. 1996; Lagache et al. 1998; Arendt et al. 1998; Schlegel, Finkbeiner, & Davis 1998; Finkbeiner, Davis, & Schlegel 1999). This characterization of the diffuse Galactic emission was a key step in the discovery of the cosmic far-infrared background (CFIRB) with the Diffuse Infrared Background Experiment (DIRBE) and the Far-Infrared Absolute Spectrophotometer (FIRAS) (Puget et al. 1996; Hauser et al. 1998). The present uncertainties in the CFIRB spectrum at $\lambda > 100$ μm are still set by the limits of our understanding of the Galactic contribution to the sky emission. In this paper we review the main results of large scale studies of the far-IR ($\lambda > 100$ μm) Galactic emission from the solar neighborhood interstellar medium obtained with the IRAS and COBE data. We give further insight into the changes of dust emission

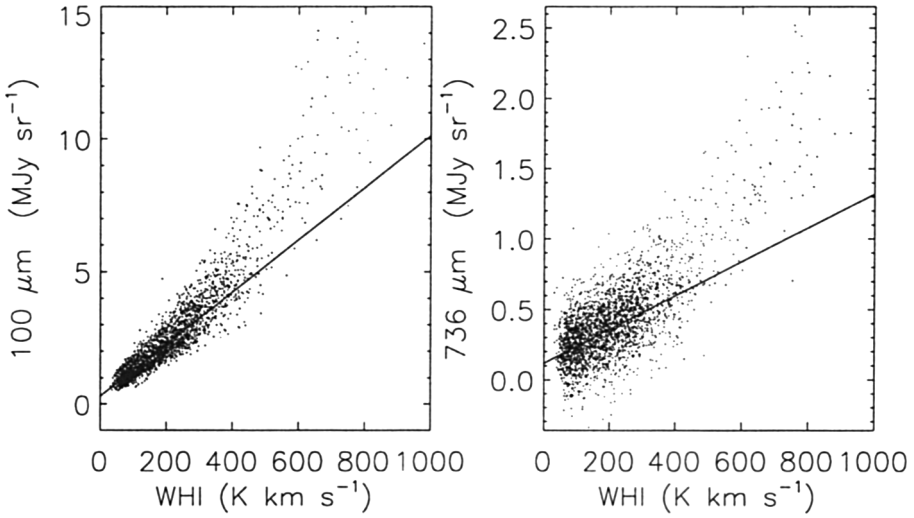

Figure 1. Pixel by pixel comparison of far-IR COBE dust maps with 21 cm line emission from HI integrated in velocity from the Leiden-Dwingeloo survey. Left: 100 μm map smoothed with the FIRAS 7° beam. Right: FIRAS data averaged around the mean wavelength $\lambda = 736\,\mu$m (see Boulanger et al. 1996 for details)

properties from atomic to molecular gas by presenting higher angular resolution sub-mm observations of pieces of the Polaris and Taurus molecular clouds obtained with the balloon borne PRONAOS experiment.

2. Dust/Gas Correlation at High Galactic Latitude

The determination of the Galactic component relies on the existence of a spatial correlation between gas and dust, and thus of gas emission lines with the associated dust emission. The slope of these correlations, the IR emission per unit gas column density, is used to estimate the Galactic emission in regions of low interstellar column densities used to determine the intensity of the CFIRB. An accurate estimate of the Galactic emission is particularly critical for the determination of the CFIRB intensity around 140 μm where the Galactic dust emission spectrum peaks. The correlation which has been most extensively investigated is that between infrared emission and the 21 cm line from atomic hydrogen. H_α observations, including the recently completed Wisconsin H_α mapper (WHAM) survey, have prompted several searches for an emission component associated with diffuse ionized gas.

2.1. Far-IR Emission Associated with HI and H_2 Gas

Several studies based on IRAS data have shown that the 100 μm emission away from the Galactic plane and away from molecular clouds is correlated with the distribution of neutral atomic gas as traced by the HI line (e.g., Boulanger

https://doi.org/10.1017/S0074180900225874 Published online by Cambridge University Press

& Pérault 1988). This correlation analysis has been extended to the whole dust spectrum using data from the DIRBE and FIRAS instruments on board COBE (Boulanger et al. 1996; Arendt et al. 1998). The correlation is linear and particularly tight where the HI column density is lower than 5×10^{20} H cm^{-2}. For higher column densities, there is a significant excess of IR emission above the extrapolation of the low column density IR-HI linear correlation. The 5×10^{20} H cm^{-2} column density corresponds to the threshold above which H_2 UV observations show that a significant fraction of the gas is molecular (Savage et al. 1977). This excess is thus attributed to IR emission from dust associated with molecular gas. This interpretation is also supported by the general coincidence of IR excess with CO emission. However, the correlation between IR excess and CO emission is quantitatively poor. This is not surprising because abundance, excitation and optical depth effects make the CO emission a poor quantitative tracer of the spatial distribution of molecular hydrogen at high Galactic latitude (e.g., Meyerdierks & Heithausen 1996) .

The far-infrared/HI correlation shows that dust and gas are well mixed and that, at high Galactic latitude, the intensity of dust heating is quite homogeneous. However, the scatter in the DIRBE 100 μm - HI correlation at low column densities is larger than the noise in the data (Boulanger et al. 1996 and Figure 1 - note that the larger scatter in the sub-mm plot is within the noise of the FIRAS data). There are several plausible explanations for this scatter: IR emission from ionized or molecular gas and variations in the heating radiation field, in dust properties and/or in the dust-to-gas ratio. Present data do not permit disentangling these effects. With the assumption of fixed dust properties, variations in dust heating would translate into variations in dust temperatures. However, in the low column density parts of the sky, the signal-to-noise ratio of the DIRBE data, much lower in the 140 and 240 m bands than at 100 μm, is insufficient to look for such temperature variations. In the next subsection we discuss another potential explanation by reviewing searches for IR emission from the warm ionized medium (WIM).

2.2. IR Emission from the Warm Ionized Medium

Dispersion measures in the direction of pulsars at large distances from the Galactic plane show that 30% of the gas in the solar neighborhood is low density ($n_e \sim 0.1\,cm^{-3}$) ionized gas, not directly associated with ionizing stars and known as the warm ionized medium (Reynolds 1989). Since fast shock waves propagating in the low density components of the ISM are theoretically predicted to be effective in eroding and shattering interstellar grains (Jones, Tielens, & Hollenbach 1996), the dust abundance and size distribution in the WIM could be quite different from that in HI clouds. Depletion measurements show that grains are partially but not fully destroyed in warm low density gas (Savage and Sembach 1996). The contribution from the WIM to the Galactic far-infrared emission has been a vexing issue since the first attempt to look for it in the IRAS data (Boulanger & Pérault 1988).

Several attempts (e.g., Kogut 1997; McCullough 1997) to identify IR emission from the WIM have been carried out by correlating the far-IR and H_α maps ignoring the dominant contribution from dust in the HI gas. In this approach, the HI emission component that could be accounted for by including HI data

https://doi.org/10.1017/S0074180900225874 Published online by Cambridge University Press

in the correlation analysis comes in as a source of noise. Further, any positive correlation found in such an analysis is inconclusive because it could result from some degree of correlation between HI and HII gas. One is really left with the difficult task of looking for an IR counterpart to HII gas spatially uncorrelated with HI gas, in the residuals of the IR-HI correlation. Lagache et al. (1999) have shown that structure in the WIM uncorrelated with HI could explain the observed scatter in the ratio between far-IR and HI emission at high Galactic latitude, for an abundance of dust in the WIM similar to that in the HI gas and proportions of uncorrelated and correlated H II gas of 70% and 30%. But this is only a tentative determination of the WIM IR emission since this work is based on a simulation and not a real image of the WIM spatial distribution. Two groups have correlated the far-IR DIRBE maps simultaneously with HI and H_α observations over two different sky patches with diverging conclusions. Arendt et al. (1998) found no correlation, while Lagache et al. (2000) found a statistically significant correlation at a level above the upper limit of Arendt et al. The only reservations one can have on the statistical significance of the Arendt et al. analysis comes from the limited size of their map (100 square degrees with a 1° beam). A larger scale study around the same area with the WHAM data could solve the discrepancy between the two studies. Converting the H_α emission in a column density estimate based on a mean WIM electron density $< n_e > \sim 0.08\,\mathrm{cm}^{-3}$, Lagache et al. (2000) derive from their correlation an estimate of the IR emission per hydrogen atom comparable in the WIM to that in the HI gas. We refer to Puget and Lagache's paper in this volume for the impact of the WIM contribution on the CFIRB determination.

3. Spectral Energy Distribution of Dust Emission

The average emission spectrum measured for dust at high latitude is presented in Figure 2. In particular, the long wavelength spectrum results from a linear correlation of the FIRAS and HI data at low HI column densities. This spectrum is well fitted by a single Planck curve with an emissivity proportional to ν^2 and $T_{dust} = 17.5\,\mathrm{K}$ (Boulanger et al. 1996). Note, however, that this fit does not fully account for the 3 mm DMR measurement by Kogut, Banday, & Bennett (1996). The most recent determination of the dust emissivity per H atom takes into account the effect of infrared emission from dust in the warm ionized medium on the infrared/HI correlation analysis (Lagache et al. 1999). Its value, $\tau_\lambda/\mathrm{N_H} = (8.7 \pm 0.9) \times 10^{-26}\,(\lambda/250\,\mu\mathrm{m})^{-2}\ \mathrm{cm}^2$ for $\lambda > 250\,\mu$m, is remarkably close to the value obtained by Draine and Lee (1984) for a mixture of compact graphite and silicate grains. Since the existence of crystalline graphite grains in interstellar space is disputed (Jones 2001), this agreement might be fortuitous and not the right physical interpretation of the data in terms of the nature of large dust grains.

By averaging FIRAS spectra over a larger portion of sky out of the Galactic plane but including nearby molecular clouds, Finkbeiner et al. (1999) convincingly showed that the one temperature fit can be very significantly improved by including a second emission component with a low temperature ($T \sim 9\,\mathrm{K}$) and an IR/visible emissivity ratio one order of magnitude larger than that of the warmer component. In this data fitting, the two temperatures vary with

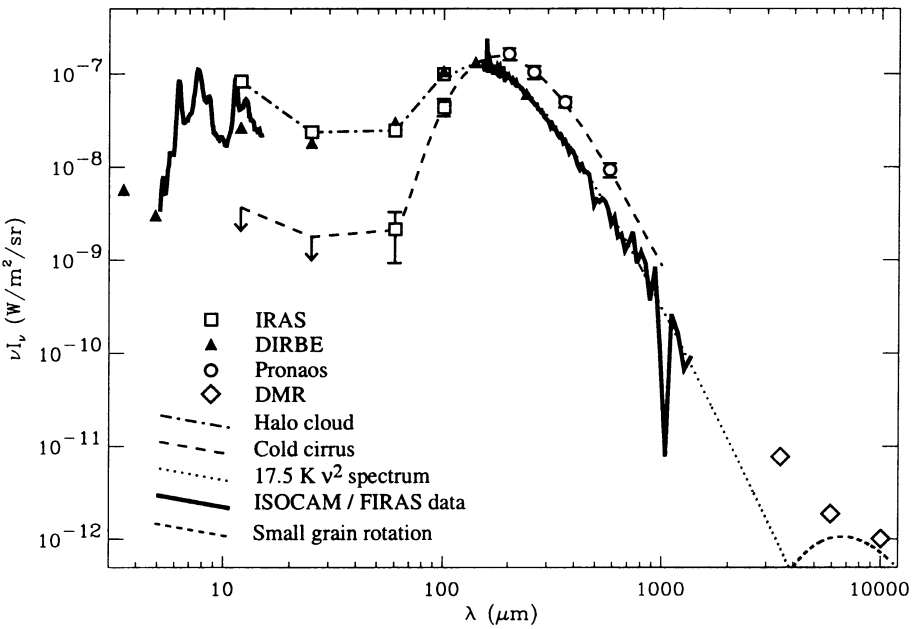

Figure 2. Mean high latitude dust spectrum (DIRBE, ISOCAM, FIRAS and DMR data). Variations in observed dust SEDs around the mean spectrum are illustrated by the spectrum of the Polaris molecular cirrus (cold cirrus, data from Bernard et al. 1999) and a cloud of comparable visible opacity [$A_V(\mathrm{max}) \sim 2$] with bright 12 μm emission in Chamaeleon (halo cloud)

https://doi.org/10.1017/S0074180900225874 Published online by Cambridge University Press

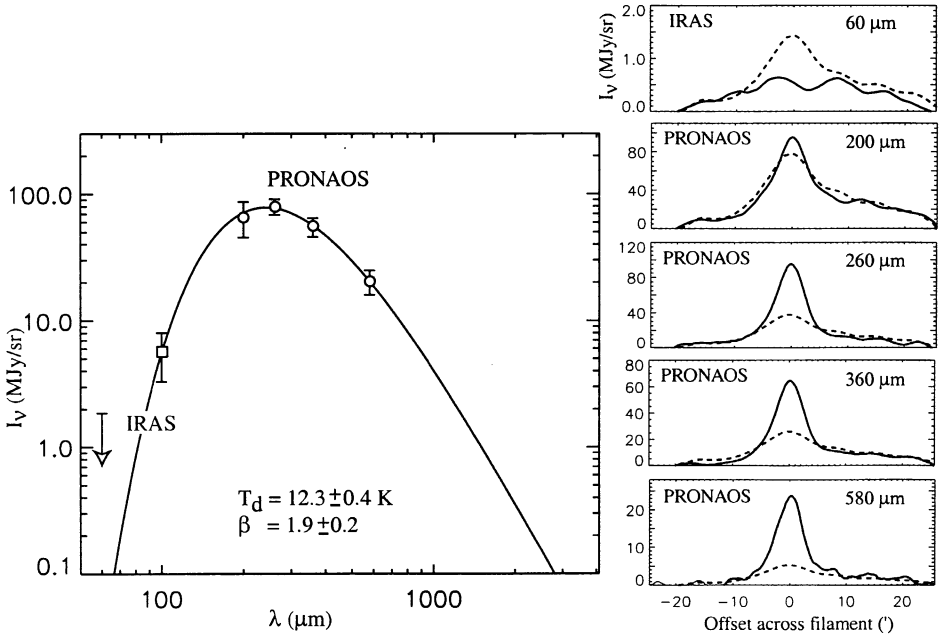

Figure 3. Spectrum of cold dust in a filament in Taurus (PRONAOS data from Stepnik et al. 2001). The difference in dust spectra between the filament and the more diffuse medium surrounding it is illustrated in the brightness cuts. In each cut, the dashed curve is the IRAS 100 μm brightness profile scaled with the color ratios of the extended emission at the basis of the filament.

https://doi.org/10.1017/S0074180900225874 Published online by Cambridge University Press

sky position within a fixed relation determined by the equation determining the equilibrium temperature of each dust component. It is unclear what the physical significance of the cold temperature component may be, and in particular if it truly represents the emission from grains which are cold because they have a large far-IR emissivity.

4. Cold Dust in Molecular Gas

After being released by the outflows of evolved stars, dust is subject to processing in the ISM through gas-grain, grain-grain and photon-grain interactions. The degree and nature of the processing (e.g., grain coagulation or shattering in grain-grain collisions) depends on the rate and energy of these interactions which are both related to the density structure and dynamics of the ISM. Dust grains decouple from gas motions where their friction time (time for a grain to have collided with its own mass of gas) is larger than the time-scales over which the gas velocity changes significantly. This applies not only to shocks, where grains do not follow the immediate velocity change of the gas, but also in turbulent clouds. One should thus not be surprised to observe that dust properties vary within the ISM. These variations can be of importance for predicting the dust emission at mm wavelengths in CMB observations. They also limit the sky area usable for the determination of the spectrum and angular structure of the CFIRB.

The IRAS and COBE sky images show that the SED of the dust emission varies within the ISM, and in particular from the diffuse atomic medium to molecular clouds. The IRAS data have revealed variations in the emission from aromatic hydrocarbons and very small grains at 12, 25 and 60 μm, relative to that from large dust grains at 100 μm (Boulanger et al. 1990; Bernard, Boulanger, & Puget 1993). In particular, emission from small particles is not detected towards the dense gas traced by the millimeter transitions of ^{13}CO (Laureijs, Clark, & Prusti 1991); the difference between the 100 and 60 μm IRAS images have been successfully used to trace the distribution of dense gas in the solar neighborhood (e.g., Abergel et al. 1994) The IRAS SED variations have been related to a drop in the abundance of small grains from the diffuse ISM to dense gas. The long wavelength bands of DIRBE opened the possibility of determining the temperature of large dust grains. Lagache et al. (1998) combined the far-IR DIRBE bands and the 60 μm data to separate along each line of sight the emission associated with the diffuse ISM and dense gas where both are present. The results of this separation show that the dust associated with the dense gas, as traced by the difference between the 100 and 60 μm brightnesses, is systematically colder ($T \sim 15$ K) than dust in the diffuse atomic interstellar medium ($T \sim 17.5$ K). Schlegel et al. (1998) have traced temperature variations in a different way. They used the ratio between the 100 and 240 μm DIRBE images to measure a dust temperature for each DIRBE pixel. The important question left open by both analyses is the origin of the temperature variations. Do they trace variations in the intensity of the heating stellar radiation field or variations in dust properties? An answer to this question is being provided by observations with higher angular resolution.

Balloon borne sub-mm observations are bringing additional evidence for the existence of cold dust associated with molecular clouds of moderate visible opacity (e.g., Figure 3, Bernard et al. 1999; Stepnik et al. 2001). With the few arcminutes resolution of these observations, it is possible to model the effect of the radiation field attenuation, associated with dust extinction, on dust temperatures. By combining the IR data with A_V measurements in a model of IR emission from clouds, Bernard et al. and Stepnik et al. convincingly show that the cold dust temperatures cannot be accounted for by the attenuation of the interstellar radiation field. They conclude that a variation in the ratio between dust far-IR emissivity and visible opacity by a factor of 3 is required to explain the cold dust temperatures in the Taurus and Polaris clouds. For the Polaris cloud, the same change in emissivity is inferred from the comparison of dust far-IR opacities with A_V values derived from star counts (Cambresy et al. 2001). These variations in the τ_{FIR}/A_V ratio questions the validity of the A_V map derived from dust opacities by Schlegel et al. 1998 in regions of moderate opacity ($A_V \sim 1$ and higher) where cold dust is present.

5. Conclusion

IR and sub-mm observations from space and balloons are prompting much progress in our understanding of the emission from interstellar dust at far-IR and sub-mm wavelengths. This progress has been associated with the discovery of the CFIRB. It contributes to our understanding of the nature of dust grains and their evolution with physical conditions in the interstellar medium. This understanding will ultimately also be important to achieve the optimal sensitivity in studies of the structure of the cosmic microwave background.

References

Abergel, A., et al. 1994, ApJ, 423, L59

Arendt, R. G., Odegard, N., Weiland, J. L., et al. 1998, ApJ, 508, 74

Bernard, J.-P., Boulanger, F., & Puget, J.-L. 1993, A&A, 277, 609

Bernard, J. P., Abergel, A., Ristorcelli, I., et al. 1999, A&A, 347, 640

Boulanger, F., & Pérault, M. 1988, ApJ, 330, 964

Boulanger, F., Falgarone, E., Puget, J.-L., & Helou, G. 1990, ApJ, 364, 136

Boulanger, F., Abergel, A., Bernard, J.-P., et al. 1996, A&A, 312, 256

Cambresy, L., Boulanger, F., Lagache, G., & Stepnik, B. 2001, submitted to A&A

Draine, B. T., & Lee, H. M. 1984, ApJ, 285, 89

Finkbeiner, D. P., Davis, M., & Schlegel, D. J. 1999, ApJ, 524, 867

Hauser, M. G., Arendt, R. G., Kelsall, T., et al. 1998, ApJ, 508, 25

Jones, A. P., Tielens, A. G. G. M., & Hollenbach, D. J. 1996, ApJ, 469, 740

Jones, A. P. 2001, submitted to A&A

Kogut, A., Banday, A., & Bennett, C. L. 1996, ApJ, 464, L5

Kogut, A. 1997, AJ, 114, 1127

Lagache, G., Abergel, A., Boulanger, F., & Puget, J.-L. 1998, A&A, 333, 709
Lagache, G., Abergel, A., Boulanger, F., et al. 1999, A&A, 344, 322
Lagache, G., Haffner, L. M., Reynolds, R. J., & Tufte, S. L. 2000, A&A, 354, 247
Laureijs, R., Clark, F. O., & Prusti, T. 1991, A&A, 372, 185
McCullough, P. R. 1997, AJ, 113, 2186
Meyerdierks, H., & Heithausen, A. 1996, A&A, 313, 929
Puget, J. L., Abergel, A., Bernard, J. P., et al. 1996, A&A, 308, L5
Reach, W. T., Dwek, E., Fixsen, D. J., et al. 1995, ApJ, 451, 188
Reynolds, R. J. 1989, ApJ, 339, L29
Savage, B. D., Bohlin, R. C., Drake, J. F., & Budich, W. 1977, ApJ, 216, 291
Savage, B. D., & Sembach, K. R. 1996, ARAA, 34, 279
Schlegel, D. J., Finkbeiner, D. P., & Davis, M. 1998, ApJ, 500, 525
Stepnik, B., et al. 2001, submitted to A&A
Wright, E. L., Mather, J. C., Bennett, C. L., et al. 1991, ApJ, 381, 200